

Copyright © 1990, by the author(s).
All rights reserved.

Permission to make digital or hard copies of all or part of this work for personal or classroom use is granted without fee provided that copies are not made or distributed for profit or commercial advantage and that copies bear this notice and the full citation on the first page. To copy otherwise, to republish, to post on servers or to redistribute to lists, requires prior specific permission.

**ELECTRON BEAM PROBE MEASUREMENTS
OF ELECTRIC FIELDS IN RF DISCHARGES**

by

A. H. Sato and M. A. Lieberman

Memorandum No. UCB/ERL M90/49

6 June 1990

CLOVER PAGE

**ELECTRON BEAM PROBE MEASUREMENTS
OF ELECTRIC FIELDS IN RF DISCHARGES**

by

A. H. Sato and M. A. Lieberman

Memorandum No. UCB/ERL M90/49

6 June 1990

ELECTRONICS RESEARCH LABORATORY

College of Engineering
University of California, Berkeley
94720

TITLE PAGE

**ELECTRON BEAM PROBE MEASUREMENTS
OF ELECTRIC FIELDS IN RF DISCHARGES**

by

A. H. Sato and M. A. Lieberman

Memorandum No. UCB/ERL M90/49

6 June 1990

ELECTRONICS RESEARCH LABORATORY

College of Engineering
University of California, Berkeley
94720

Electron Beam Probe Measurements of Electric Fields in RF Discharges

A.H. Sato
Department of Physics

and

M.A. Lieberman
Department of Electrical Engineering and Computer Sciences

University of California, Berkeley, CA 94720

Abstract

An electron beam probe has been used to make time and space resolved measurements of the electric field in a parallel plate rf discharge. Measurements were taken at a time resolution of 5ns and a field resolution of $\pm 1\text{V/cm}$ at increments of 0.32cm from the powered electrode. The detection method provides the weighted average of the electric field along the beam trajectory. Measurements of fields less than 20V/cm were made throughout the entire discharge. Data were obtained for 13.6MHz argon discharges at 2.3mtorr and 20mtorr, and at rf voltage amplitudes of 100V and 600V at each pressure. The data for the 2.3mtorr, 600V case show 1) that a propagating double layer forms during the collapse of the sheath, 2) that the field near the electrode points in toward the plasma at the extreme collapse of the sheath, 3) that the collapse and expansion of the sheath proceeds asymmetrically for measurable field values, and 4) that the trajectory averaged electric field in the plasma has an anomalous phase shift and magnitude. Similar phenomena are observed for the remaining three discharge cases.

I. Introduction

The electric field profile in gas discharges has long been of interest to those seeking to understand their structure and operation. As early as 1909 workers used electron beam probes to measure the electric field in dc glow discharges to further their understanding of the generation, excitation, and transport of charged particles in that system.^{1,2} The electrostatic structure of dc discharges remains of interest in recent years.^{3,4}

Interest in rf discharges began in the 1920's, and in the 1960's much work using electron beam probes was done to investigate the sheath-plasma system in rf perturbed dc discharges⁵ and rf self-sustained discharges.⁶ The 1960's also saw increased interest in rf discharges for sputtering, and more recently in deposition and patterning processes in the microelectronics industry. Knowledge of the electric field is important since it provides a beginning point in understanding surface processes and discharge chemistry. Observations of time and space resolved plasma induced emission in discharges driven at 13MHz has brought attention to the possible importance of electrostatic modes in the plasma and sheath boundary phenomena.^{7,8,9} Rf discharges are interesting because the time varying sheath fields provide a collisionless mechanism by which plasma electrons may gain energy. Such a notion was evident as early as 1946.¹⁰ This was further developed by Godyak¹¹ for rf discharges, and has been further explored in recent years.^{12,13} Electric field measurements were addressed again by Gottscho¹⁴, using laser induced fluorescence spectroscopy. Field measurements were reported in the sheath of a 10MHz discharge with a resolution of $\pm 50\text{V/cm}$.

We report here on measurements of electric field in capacitive rf discharges in parallel plate configuration, made using an electron beam probe. This technique provides time and space resolved data for the mean electric field perpendicular to the powered electrode for rf driving frequencies up to 13.6MHz with a field resolution of $\pm 1\text{V/cm}$. We have used this probe in argon discharges at pressures up to 20mtorr. Here we describe the electron beam probe measurement system, and provide data acquired for 2.3mtorr and 20mtorr discharges driven at 100V and 600V at 13.6MHz. We present some evidence for 1) a propagating double layer in the contracting sheath, 2) asymmetric contraction and expansion of a constant field boundary in the sheath,

3) an electric field near the powered electrode pointing in toward the plasma when the sheath has totally collapsed, and 4) an anomalous phase shift and magnitude of the electric field in the plasma.

II. Experimental Apparatus

The RF Discharge System

An argon discharge is generated within an aluminum cylindrical vacuum chamber having an inner diameter of 12 inches. (See Figure 1). There are pistons at each end of the cylinder on which are mounted nine inch diameter copper electrodes. The cylindrical wall of the vacuum chamber and one of the electrodes is electrically grounded. The other electrode is driven by the rf power supply. A grounded guard electrode (consisting of a band of 1/16 inch thick copper, with an inner diameter of about 9.3inches) is placed around the powered electrode in order to control fringe fields from the powered electrode. The discharge length is fixed by the separation between the piston mounted electrodes. For the experiments described here, this was kept at three inches. Because the vacuum chamber wall and one electrode are grounded together, the discharge is driven asymmetrically and during operation a dc bias develops across the electrodes.

RF power is supplied by a Model A300 Power Amplifier (Electronic Navigation Industries, Inc.) through an L-type matching network. RF power is measured using a Model 43 wattmeter (Bird Electronic Corporation). Typical plasma densities vary from 10^9 to 10^{10}cm^{-3} as the absorbed power varies from a few watts to 100 watts, for neutral pressures of a few to tens of millitorr. The oscillating part of the rf voltage is monitored through a capacitive divider mounted at the powered electrode, and the dc component of the voltage on the powered electrode is monitored through a low-pass filter mounted at the output of the power amplifier.

The Electron Beam

The electron beam is supplied by a Type SW67 electron gun (Southwest Vacuum Devices, Inc). The

gun has an oxide coated cathode, and is operated in an auxiliary vacuum system which maintains a pressure of 10^{-7} torr. This is required to prevent rapid degradation of the cathode from ion bombardment. A beam energy of 8kV is used for this experiment. The electron gun vacuum chamber is connected to the rf discharge vacuum chamber through a differential pumping section. (See Figure 2a). Two 0.5mm diameter apertures separate both vacuum chambers from the differential pumping section. The apertures are spaced 12.2cm apart and also serve to collimate the beam. After collimation the beam current is 4-10 microamps.

Two sets of electrostatic deflection plates are positioned within the differential pumping section. They are used to steer the beam through the two apertures and, more importantly, to control the entrance angle of the electron beam into the discharge. Figure 3 illustrates an idealized version of this technique. The two apertures of the differential pumping section are aligned along a line passing through the center of the rf discharge chamber and parallel to the powered electrode. The electron beam enters the first aperture along this line and would pass through the second aperture in the absence of any bias across the deflection plates; for no bias the exit angle is zero. Consider how biasing the deflection plates enables one to control the exit angle of the beam. In Figure 3 the uniform electric fields E_1 and E_2 exist in two regions of equal length L . One may show that the condition for the beam to pass through the second (left) aperture is

$$E_2 = -3E_1 \quad (1)$$

and that the exit angle of the beam at the second aperture is

$$\tan \theta_2 = \frac{E_1 L}{V_b} \quad (2)$$

where V_b is the beam voltage.

Region 3 of length L_3 beyond the second aperture is filled with a uniform electric field E_3 . This represents the electric field in the rf discharge chamber. A beam detector is placed at the end of region 3, directly opposite and in line with the pair of apertures. In the absence of any bias on the deflection plates and any electric field in region 3, the beam would strike this detector. For this uniform field example one may

show that the beam will strike the detector if the entrance angle θ_2 and field E_3 satisfy the relation

$$\tan\theta_2 = \frac{1}{4} \frac{E_3 L_3}{V_b} \quad (3)$$

Combining (2) and (3), the bias field E_1 on the first deflection plate is proportional to the field in region 3, the constant of proportionality depending on the aspect ratio L_3/L , independent of the beam voltage V_b .

The actual relation between the necessary deflection plate biases and the field E_3 is complicated by drift spaces and nonuniform electric fields. Therefore, a calibration was performed to relate an averaged electric field along the beam trajectory to the deflection plate biases. The powered and grounded electrodes were spaced 3cm apart, a known dc voltage was imposed on the powered electrode, and the deflection plate biases which brought the beam to the detector were recorded. In fact, the relation between E_1 and E_2 is given roughly by the factor of -3, as predicted by (1).

The detector is a piece of Pilot B scintillating plastic covered on one face with a 2000 angstrom thick layer of aluminum.¹⁵ The scintillating plastic has a decay time of 1.8ns. A 5 micron wide slit is placed in front of the scintillating plastic to provide resolution of the beam profile. In this arrangement the finite beam diameter places a limit on the measureable field resolution. The beam current profile is roughly gaussian with a full width at half maximum of 2V/cm.

The detection method was tested by applying an rf voltage applied across the electrodes in the absence of a discharge. In the presence of the rf voltage, the beam will strike the detector when the trajectory averaged field value assumes that value consistent with the deflection plate biases. The time of this event is marked by peak fluorescence in the Pilot B. This yields the electric field as a function of time at some axial location in the discharge chamber. The rf vacuum field test gave good agreement between the known rf sine wave and the measured electric field values. This exercise also allows one to determine the time delay between the rf voltage and the photomultiplier tube signal.

The transit time of the beam across the discharge chamber is about 5ns. In these experiments the period of the rf voltage is 73ns. One may regard the measured electric field value as being a weighted average

of the field along the trajectory. The spatial resolution along the axial direction is limited by the curvature in the beam trajectory. A rough estimate for this apparatus is an excursion from the undeflected path of 1mm per 10V/cm. A figure approximately half this value was found by moving the powered electrode relative to the beam apertures until the beam was cut off.

As shown in Figure 2b, the optical signal from the scintillator is fed through a fiber optic light guide to a R647-04 photomultiplier tube (Hamamatsu Corp.). The output of the photomultiplier is fed to a Model 6954B-100 pulse preamp (Phillips Scientific), which then feeds into a Model SR250 Gated Integrator and Boxcar Averager (Stanford Research Systems). Signal averaging was used to overcome the shot noise inherent in the scintillator output at the low beam currents used. Optical isolation of the photomultiplier, and care in construction of the triggering circuit to the boxcar are provided to prevent pickup of noise generated by the discharge.

III. Experimental Measurements

Figure 4 shows the electric field profiles at various times (labeled a,b,c,d,e,f) spaced 5ns apart for a discharge in argon at a neutral pressure of 2.3 mtorr and an rf voltage amplitude of approximately 600V. The data were originally acquired as the time of occurrence of a specified field at a fixed axial position, with the field intervals chosen to be in approximately 3.3V/cm steps between -30V/cm and +10V/cm. Field values at time intervals of 5ns were obtained from this original data by interpolation. Finally, the field values from all axial positions were regrouped to form the plots in Figure 4. The discharge length is 7.62cm but only the field profiles within the first 3cm from the powered electrode (located at 0cm) are shown. A negative electric field value means the field vector is pointing from the plasma to the electrode. Also shown in Figure 5 is the rf voltage, with markers showing the times at which field profiles in Figure 4 are given. Only the oscillating part of the rf voltage is shown, as measured through a capacitive divider. The total voltage on the powered electrode has, in addition, a negative dc component so that the positive peaks in the rf waveform in Figure 5 correspond to minimum total sheath voltages.

The maximum field magnitude that can be reliably measured is 20V/cm for this 600V discharge. The beam travels on an arc that is characterized by a maximum displacement from the undeflected path. This displacement increases as the measured electric field value increases. This presents a problem in regions where the axial field gradient is substantial and the field magnitude being detected exceeds 20V/cm. In such cases the field varies significantly along the trajectory, and this degrades the spatial resolution of the measurement. It is for this reason that data points for field measurements greater than 20V/cm are not shown in Figure 4. In particular, the field value at 1.6cm in frames (a) and (f) of Figure 4 would be below -20V/cm.

The 600V discharge absorbed 100W and developed a dc bias of approximately -600V at the powered electrode. The plasma density was in the 10^{10}cm^{-3} range. Data were acquired at spacings of 0.32cm from the powered electrode. This spacing is at least a factor of three larger than the expected displacement of the beam for a 20V/cm field.

As the rf voltage rises from (a) to its peak value at (d), the sheath is collapsing. The net charge density, as given by Gauss' Law, is proportional to the slope of the field profile. In Figure 4, a positive slope in the profiles indicates a net positive charge density, and a negative slope implies a net negative charge density. In frames (b), (c) and (d) there is a region of negative charge density that advances toward the electrode at 0cm. The net charge density closer to the electrode is positive. These two regions form a double layer that appears to be moving toward the electrode as the sheath collapses. Near the peak (d) of the rf waveform the electric field profile assumes positive values. The electric field vector points in toward the plasma and momentarily accelerates electrons from the plasma into the electrode. As the rf voltage drops from its peak value, the sheath expands. The data (d) to (f) show that the expansion differs from the collapse. At (d) the region of negative charge density has increased in width. In the next 5ns at (e), field values of 10 to 15V/cm are found to penetrate almost the full 2cm to the maximum sheath thickness. Subsequently, the field in the sheath becomes too large to measure.

Figure 6 shows the field as a function of time at a fixed position in the sheath for the 600V discharge. Plotted points at three distances from the powered electrode appear together, along with the applied rf voltage (dashed curve). For this experiment the maximum total voltage across the sheath is roughly 1200V over 2cm,

and as the rf voltage goes through its negative peak the field should take on an extreme value of roughly -600V/cm . Since it was not possible to measure field values greater than 20V/cm , only the small field parts of the rf cycle are plotted. The appearance of positive electric field is clearly visible in this plot. It is also evident that the field at 0.32cm in the sheath is roughly in phase with the external rf voltage.

Figure 7 shows the field as a function of time at various positions in the plasma. The rf field amplitude is roughly $2.5 \pm 1\text{V/cm}$. One unusual feature in this graph is the phase lag of the electric field relative to the rf voltage (dashed curve). The phase lag in Figure 7 was verified using a capacitive probe to measure the rf component of the plasma potential¹⁶ (Figure 8). The capacitive probe was placed at 2.54cm from the powered electrode. For the 600V discharge, this is about 0.32cm from sheath boundary into the plasma. A surge in the plasma potential is visible which lags the rf voltage by greater than 90° . (The fast oscillations on the capacitive probe trace are due to ringing in the probe preamp, and are not a true feature of the original signal.)

The data that appear in Figure 4 can be used to construct graphs of the position at which a particular value of electric field occurs as time evolves. This yields information on the motion of the sheath boundary. These data appear in Figures 9 and 10 for two values of electric field. The experimental data are shown as points. The experimental rf voltage is also displayed, as well as results from a model for the sheath motion from Ref. 13. In these graphs, the electrode is at 1.9cm on the ordinate and the fully expanded sheath position is set to 0cm . This allows easier comparison with the results of Ref. 13.

IV. Discussion

There are two striking features about the electric field profiles in Figure 4. The first is the appearance of a propagating double layer. The second is the occurrence of positive electric field when the sheath has fully collapsed. Recent simulations by Alves et al.¹⁷ also show a propagating double layer. Their simulations were done for asymmetric discharges of cylindrical and spherical geometry. However the propagating double layer persisted when the electrode area ratio was 1.005 in both geometries. At larger area ratios the electric

field even became positive at the electrode. There has also been a simulation by Boswell and Morey¹⁸ that exhibited an inward pointing electric field. A more recent work by Vender and Boswell also shows a propagating double layer during the collapse of the sheath.¹⁹

In addition, Cho²⁰ has measured the potential profile using emissive probes in a 5MHz, 100V_{pp}, 0.2mtorr argon discharge, sustained by hot filaments in a multipole device at electron densities of 10^8 to 10^9cm^{-3} . A double layer formed in the sheath when the potential on the electrode reached its positive peak. At that moment, the electric field at the electrode pointed in toward the plasma.

We believe that electron inertia effects may lead to the formation of a double layer. The speed of a thermal electron is roughly $1 \times 10^8\text{cm/s}$. The characteristic sheath boundary speed is roughly $1.6 \times 10^8\text{cm/s}$ for a maximum sheath thickness of 1.9cm and an angular frequency of $8.5 \times 10^7\text{rad/s}$. In both dc and rf glow discharges a sheath electric field forms to attenuate the outward electron flux. However, in an rf discharge with such a rapidly moving sheath boundary, an additional contribution to the electric field develops to force the electrons to move along with the sheath boundary toward the electrode.

The solid curves in Figures 9 and 10 are calculations from the sheath model of Ref. 13 in which electron inertia is neglected and the rf discharge current is sinusoidal. These curves mark the position at which a particular value of the electric field occurs. Figure 9 illustrates how a double layer in the sheath can distort such curves. An electric field as low as -7.5V/cm occurs in the double layer (see Figure 4). This implies that an electric field more positive than -7.5V/cm can occur at as many as three positions in the sheath. This multiple valuedness is evident in Figure 9. This effect is not as pronounced when tracked field values are chosen that are more negative than those occurring in the double layer. An example of this is Figure 10a in which the -13.5V/cm curve is plotted.

Figure 10a illustrates a lack of symmetry in the collapse and expansion of the sheath. The collapse appears to be more gradual than the expansion. In fact, these experimental points follow the model curve, except for a delay of about 7ns (see Figure 10b). In comparison, the points marking the expansion of the sheath indicate an expansion of the -13.5V/cm location that is more rapid than the model curve. The points lead from 1.3cm to 0cm in about 5ns. This has implications for the energy electrons gain as they reflect off

the expanding sheath. Lieberman (Ref. 13) has performed an electron power absorption calculation in which the sheath boundary collapses and expands symmetrically. An estimate for the energy absorbed over an rf period was derived. The effect of the observed asymmetry in the sheath boundary motion would be to favor enhanced absorption of energy, as observed experimentally.²¹

It would have been useful to measure the field profile at larger field values, however this was not possible with the present apparatus. In Ref. 14 the field profile in the sheath of a 10MHz discharge in BCl₃ was measured, and it was observed that the sheath boundary moved in and out symmetrically. However, the LIF measurements were limited to a resolution of $\pm 50\text{V/cm}$. The sheath thickness in the BCl₃ discharge was about 3.2mm so that the sheath speed was only 1/5th of the thermal speed; hence electron inertial effects are not very important. Furthermore, the neutral pressure was 0.3torr and the voltage levels were lower than in our experiment.

Figures 6 and 7 show measurements of the electric field and potential in the plasma. The results differ in two ways from what one would expect in a cold uniform plasma. First, the field magnitudes are larger than what is predicted from cold plasma model. Secondly, the phase lag of the plasma electric field with respect to the rf voltage is different from what one would expect from a cold plasma model.

The plasma electric field can be estimated from the cold plasma dielectric function, as a first approximation. The maximum sheath thickness is 1.9cm for the 600V discharge. The amplitude for the rf electric field in the sheath is roughly 300V/cm. The dielectric function for a cold uniform plasma with collisional scattering and time variation $\sim \exp(-i\omega t)$ is

$$\epsilon = 1 - \frac{\omega_p^2}{\omega(\omega + i\nu^m)} \quad (4)$$

where the plasma frequency $\omega_p \approx 4 \times 10^9 \text{ rad/s}$ and ν^m is the electron momentum transfer collision frequency.

The collision frequency is roughly $5.9 \times 10^6 \text{ s}^{-1}$ for a 3eV maxwellian electron distribution in 2.3mtorr of argon.²¹ This is smaller than the angular frequency corresponding to a 13.6MHz rf voltage. Using (4) with

a density estimate of $\sim 5 \times 10^9 \text{cm}^{-3}$,

$$E_{\text{plasma}} = \frac{1}{\epsilon} E_{\text{sheath}} \quad (5)$$
$$\sim 0.14 \text{ V/cm}$$

Instead, an amplitude of $2.5 \pm 1 \text{V/cm}$ is observed. The reason for this discrepancy is not understood.

From (4) and the given collision frequency, one also finds that the plasma electric field should lead the sheath electric field by 176° if the rf sheath is purely capacitive. However, Figures 6 and 7 show that the plasma electric field lags the rf voltage by some angle between 90° and 180° . The sign of this phase shift is not consistent with a simple discharge model formed by capacitive sheaths and an inductive plasma. We cannot yet explain this particular phase lag.

Three other discharges differing in pressure and voltage have also been studied. A summary of the discharge properties is given in Table I. The 2.3mtorr discharge at 100V was very similar to the 2.3mtorr discharge at 600V. The only qualitative difference was the absence of a positive, or inward pointing, electric field during the extreme collapse of the sheath. Instead, the electric field remained negative at about -10V/cm at 3mm from the powered electrode.

When the discharge pressure was increased to 20mtorr, observations failed to detect a double layer moving toward the electrode during collapse of the sheath. In these discharges the sheaths are about half the thickness of sheaths at 2.3mtorr. Thus, if the propagating double layer is due to electron inertia, it is natural that the double layer would be less distinct in thinner sheaths.

Another consideration that may be important is the change in ion density profile with increasing pressure. At 20mtorr symmetric charge exchange becomes important, resulting in lower ion velocities in the sheath. Due to this decreased acceleration of the ions, the ion density should decrease more gradually toward the electrode than in a collisionless sheath. The propagating double layer represents an excess of electrons at the sheath boundary as the plasma surges towards the powered electrode. Thus the magnitude of the double layer fields must be related to the gradient in the ion density profile; a smaller gradient of the density

profile produces smaller charge imbalances. This effect can also be seen by increasing the ion mass for a fixed total dc sheath voltage, and there have been observations of this in the simulations of Ref. 17.

The 100V discharges at both pressures show an absence of positive electric field at the extreme collapse of the sheath. There may be at least three reasons for this: 1) the smaller dc sheath voltage produces a smaller ion density gradient; 2) the absolute electron densities in these weaker discharges are much lower than in the 600V discharges; and 3) the length of time electrons can contact the powered electrode increases with decreasing sheath voltage. These three factors would tend to lessen the charge imbalance and/or surge of electrons to the powered electrode at the positive peak in the rf voltage.

Acknowledgement

This work is supported by NSF Grant ECS-8517363 and DOE Grant DE-FG03-87ER13727.

References

1. J.J. Thomson, *Phil. Mag.* **18**, 441 (1909)
2. F.W. Aston, *Proc. R. Soc. Lond.* **84**, 526 (1911)
3. D.B. Graves and K.F. Jensen, *IEEE Trans. Plasma Sci.* **PS-14**, 78 (1986)
4. E.A. Den Hartog, D.A. Doughty, and J.E. Lawler, *Phys. Rev. A* **38**, 2471 (1988)
5. R.S. Harp, G.S. Kino, and J. Pavkovich, *Phys. Rev. Letters* **11**, 310 (1963)
6. J. Taillet, *Amer. J. Phys.* **37**, 423 (1969)
7. G. de Rosny, E.R. Mosburg, J.R. Abelson, G. Devaud, and R.C. Kerns, *J. Appl. Phys.* **54**, 2272 (1983)
8. A.J. van Roosmalen, W.G.M. van den Hoek, and H. Kalter, *J. Appl. Phys.* **58**, 653 (1985)
9. P. Bletzinger and C.A. DeJoseph, *IEEE Trans. Plasma Sci.* **PS-14**, 124 (1986)
10. L. Landau, *J. Phys. USSR* **10**, 25 (1946)
11. V.A. Godyak, *Sov. J. Plasma Phys.* **2**, 78 (1976)
12. M.J. Kushner, *IEEE Trans. Plasma Sci.* **PS-14**, 188 (1986)
13. M.A. Lieberman, *IEEE Trans. Plasma Sci.* **PS-16**, 638 (1988)
14. R.A. Gottscho, *Phys. Rev. A* **36**, 2233 (1987)
15. R. Lincke and T.D. Wilkerson, *Rev. Sci. Instrum.* **33**, 911 (1962)
16. N. Benjamin, *Rev. Sci. Instrum.* **53**, 1541 (1982)
17. M.V. Alves, V. Vahedi, and C.K. Birdsall, *Bull. Am. Phys. Soc.* **34**, 2028 (1989)
18. R.W. Boswell and I.J. Morey, *Appl. Phys. Lett.* **52**, 21 (1988)
19. D. Vender and R.W. Boswell, *IEEE Trans. Plasma Sci.*, to be published in 1990.
20. M.H. Cho, N. Hershkowitz, and T. Intrator, *J. Vac. Sci. Technol. A* **6**, 2978 (1988). See also Moo-Hyun Cho, Ph.D. dissertation, Nuclear Engineering and Engineering Physics, University of Wisconsin, Madison, 1988
21. G.R. Misium, A.J. Lichtenberg, and M.A. Lieberman, *J. Vac. Sci. Technol. A* **7**, 1007 (1989)

Table Captions

Table I. Comparison of the four argon discharges studied. The rf frequency was 13.6MHz in all cases, and the electrode separation was kept at three inches.

Figure Captions

Figure 1. The vacuum chamber and electrode configuration. The rf power electronics are also indicated. A: RF power supply. B: blocking capacitor and low-pass filter for DC bias measurement. C: wattmeter. D: matching network. E: capacitive divider.

Figure 2. (a) Positions of the electron gun, deflection plates, discharge chamber, and scintillating plastic. (b) Photomultiplier, boxcar averager, and trigger electronics.

Figure 3. Idealized trajectory of the electron beam. See text for discussion on the method for inferring electric field values.

Figure 4. Electric field profiles for 2.3mtorr, 600V discharge. The time for each frame is shown in Figure 5 as a marker on the rf voltage wave form.

Figure 5. Times for frames a-f in Figure 4 shown by markers on rf voltage wave form.

Figure 6. Electric field at three positions in the sheath. \circ : 0.32cm from powered electrode. \square : 0.95cm. Δ : 1.6cm. The dashed line is the rf voltage divided by 100, in units of volts.

Figure 7. Electric field at three positions in the plasma. \square : 2.2cm from powered electrode. Δ : 4.4cm. \circ : 6.7cm. Estimated error bars are indicated for the 2.2cm points. The other points have the same error bars, but are not so marked. The dashed line is the rf voltage divided by 100, in units of volts.

Figure 8. Capacitive probe measurement of oscillations in the plasma potential; this is the solid line. The dashed line is the rf voltage divided by 100. The probe was positioned 2.54cm from the powered electrode.

Figure Captions (con'd)

Figure 9. Position of the -7.5V/cm point in the field profile (points in graph). Solid curve is a model from Ref. 13. The flat portion of the solid curve marks the electrode position. The dashed line is the rf voltage divided by 600, in units of volts.

Figure 10. (a) Position of the -13.5V/cm point in the field profile (points in graph). Solid curve is a model from Ref. 13. (b) Experimental points advanced in time by 7ns.

pressure (mtorr)	rf voltage amplitude (volts)	power absorbed (watts)	maximum sheath thickness (cm)	positive electric field at electrode?	moving double layer observed?	-90° phase lag of plasma field?
2.3	600	110	1.9	yes	yes	yes
2.3	100	-4	1.6	no	yes	yes
20	600	110	1.1	yes	no	yes
20	100	-7	0.95	no	no	yes

TABLE I.

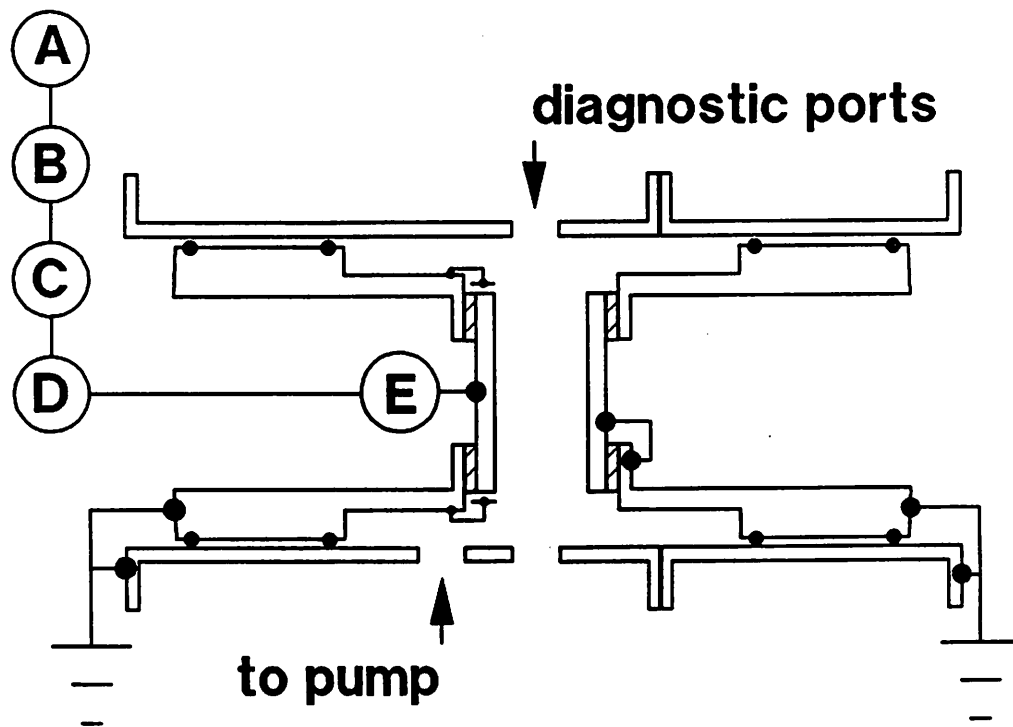


Figure 1

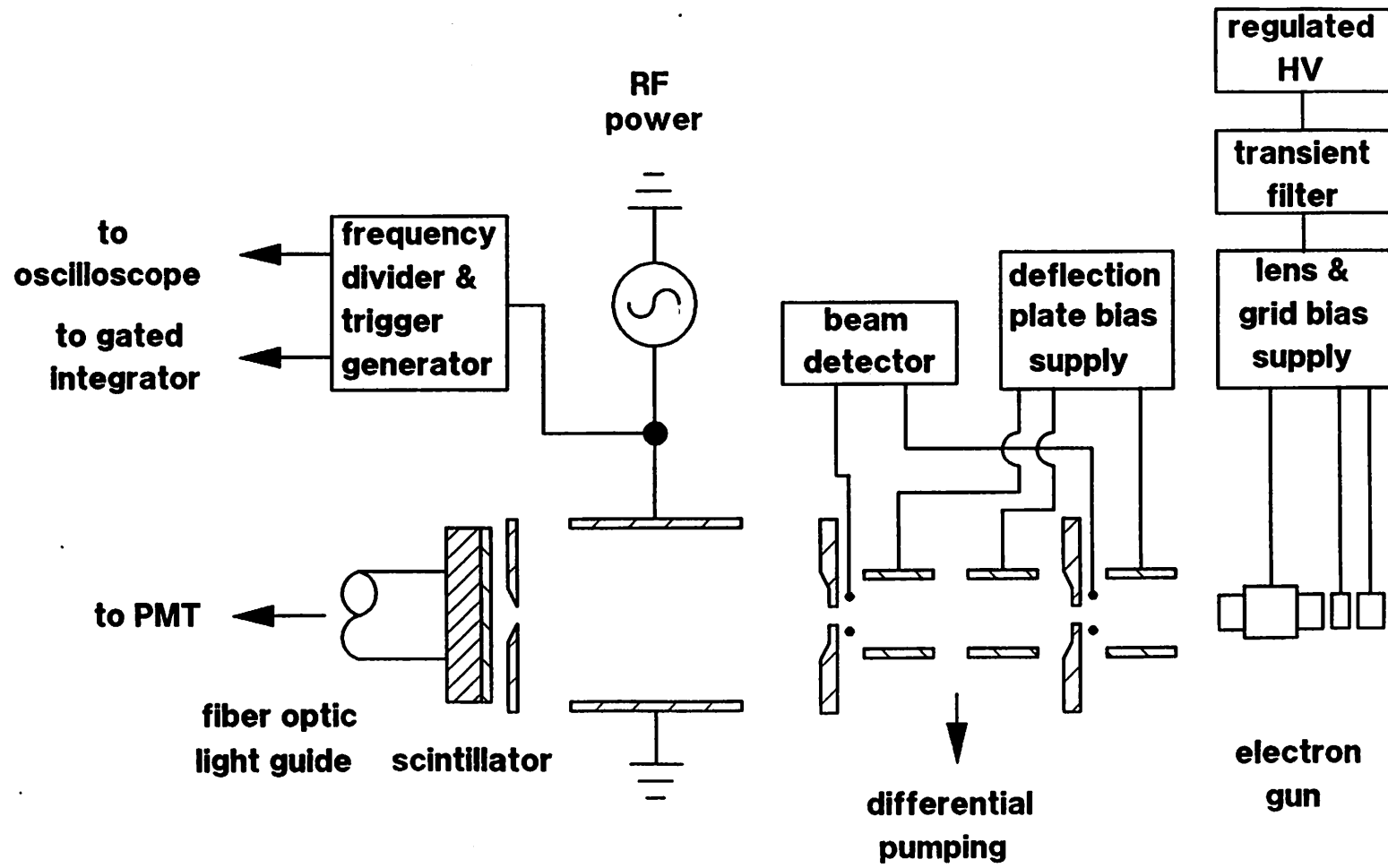


Figure 2a

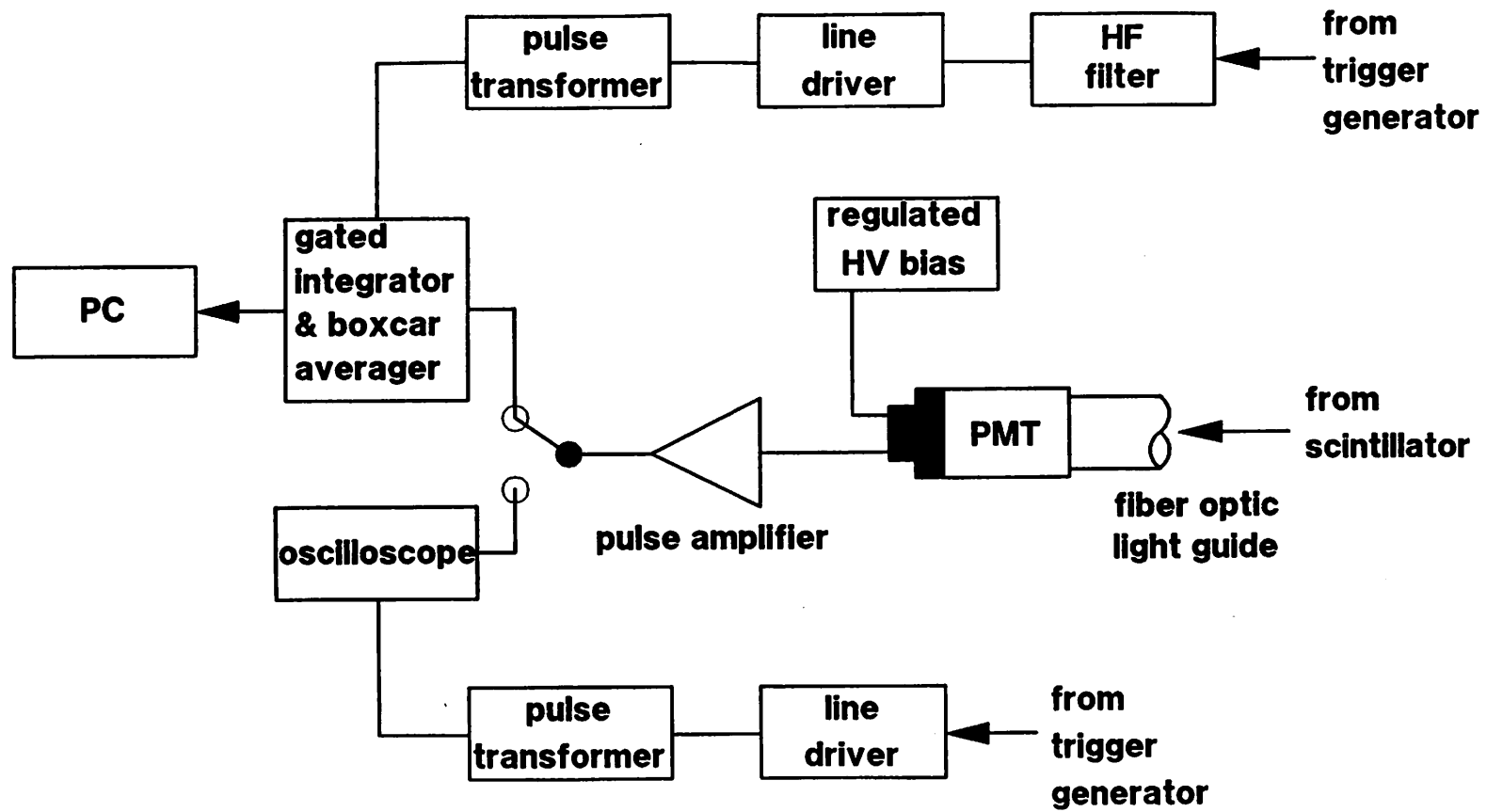


Figure 2b

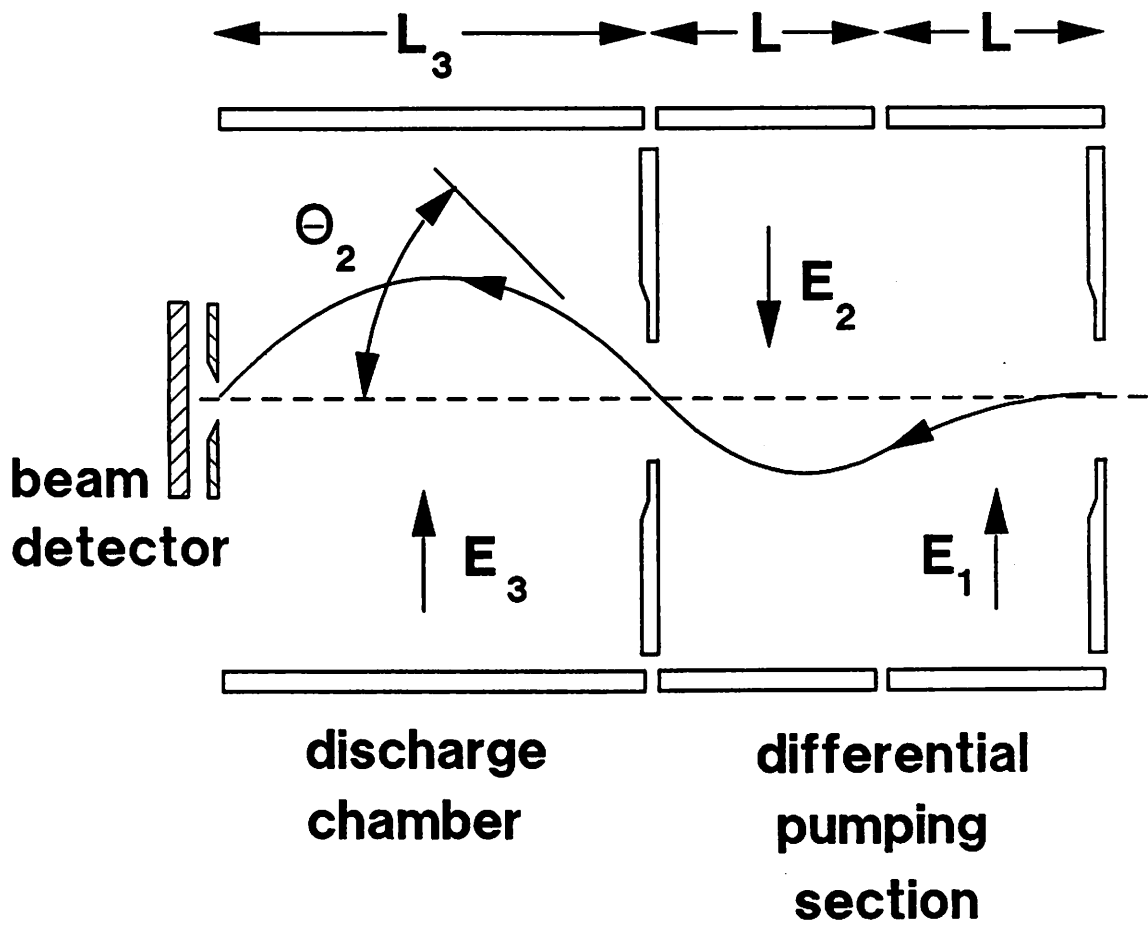


Figure 3

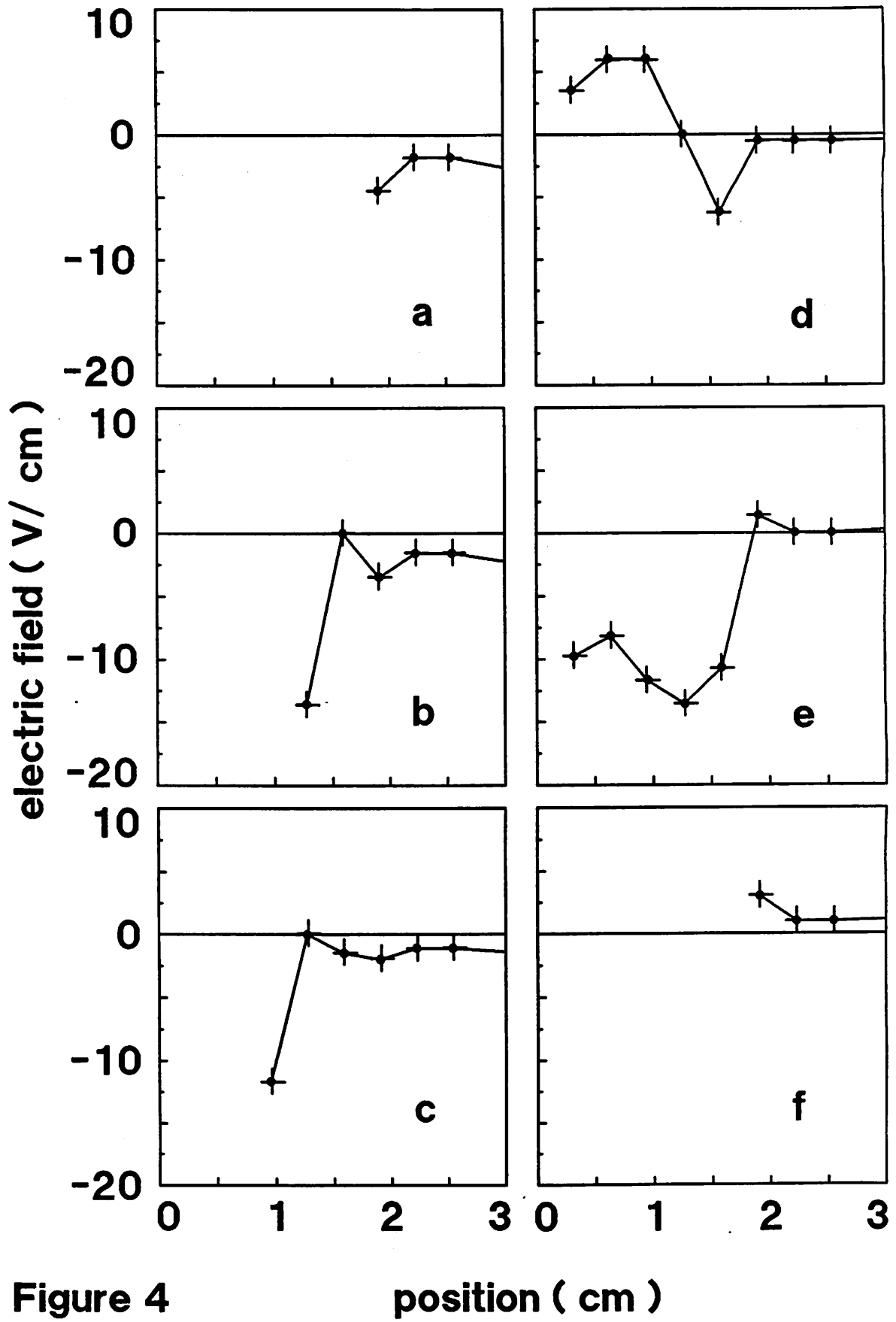


Figure 4

position (cm)

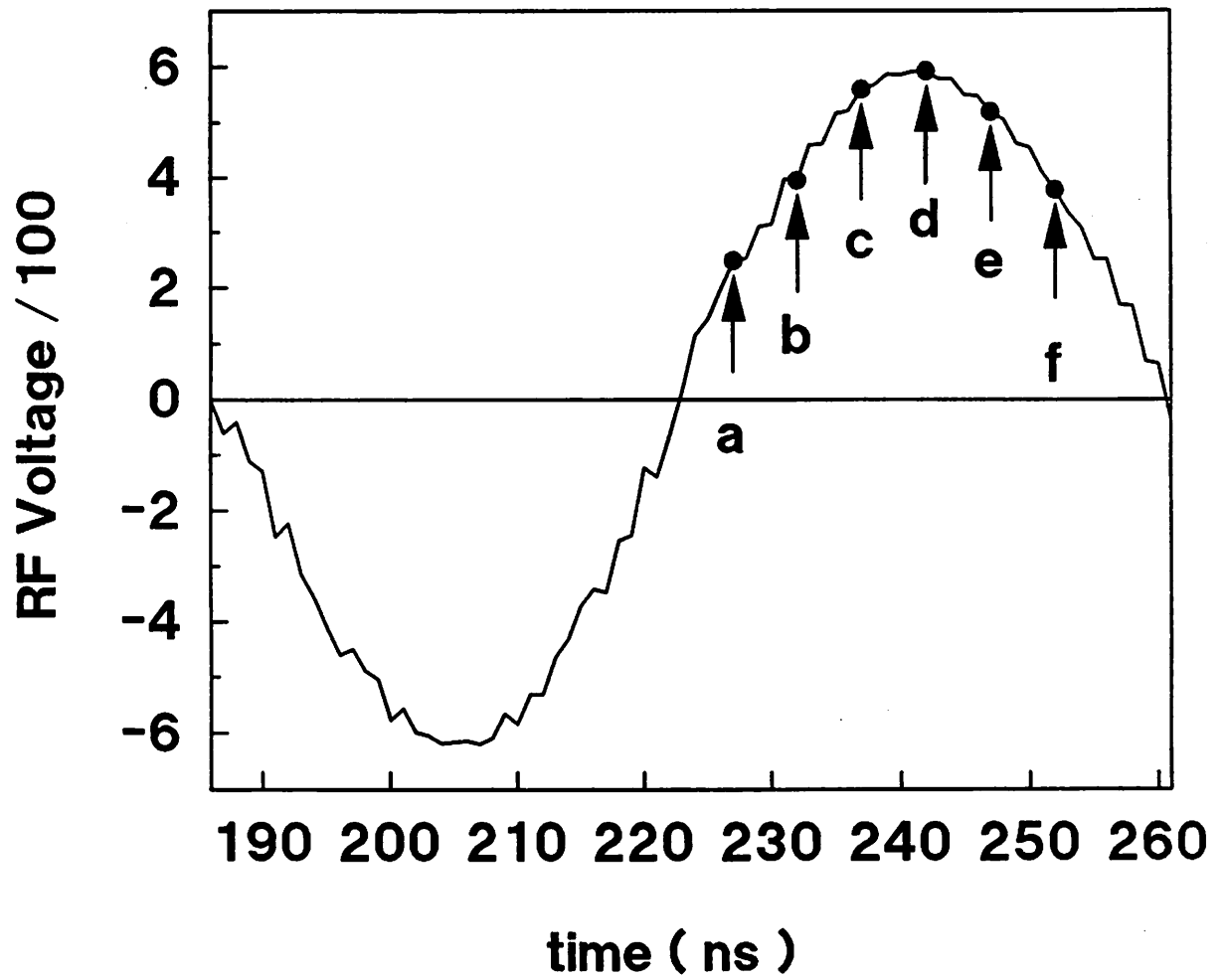


Figure 5

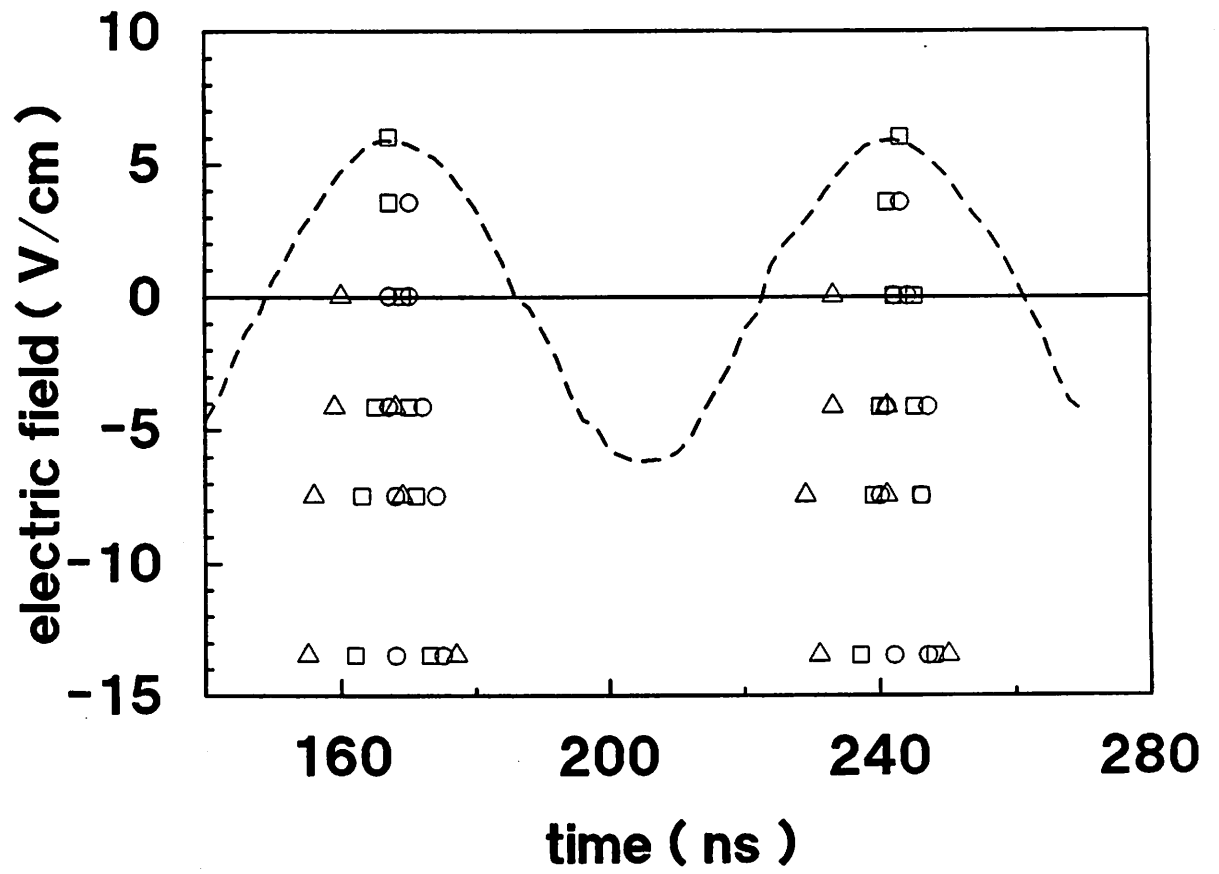


Figure 6

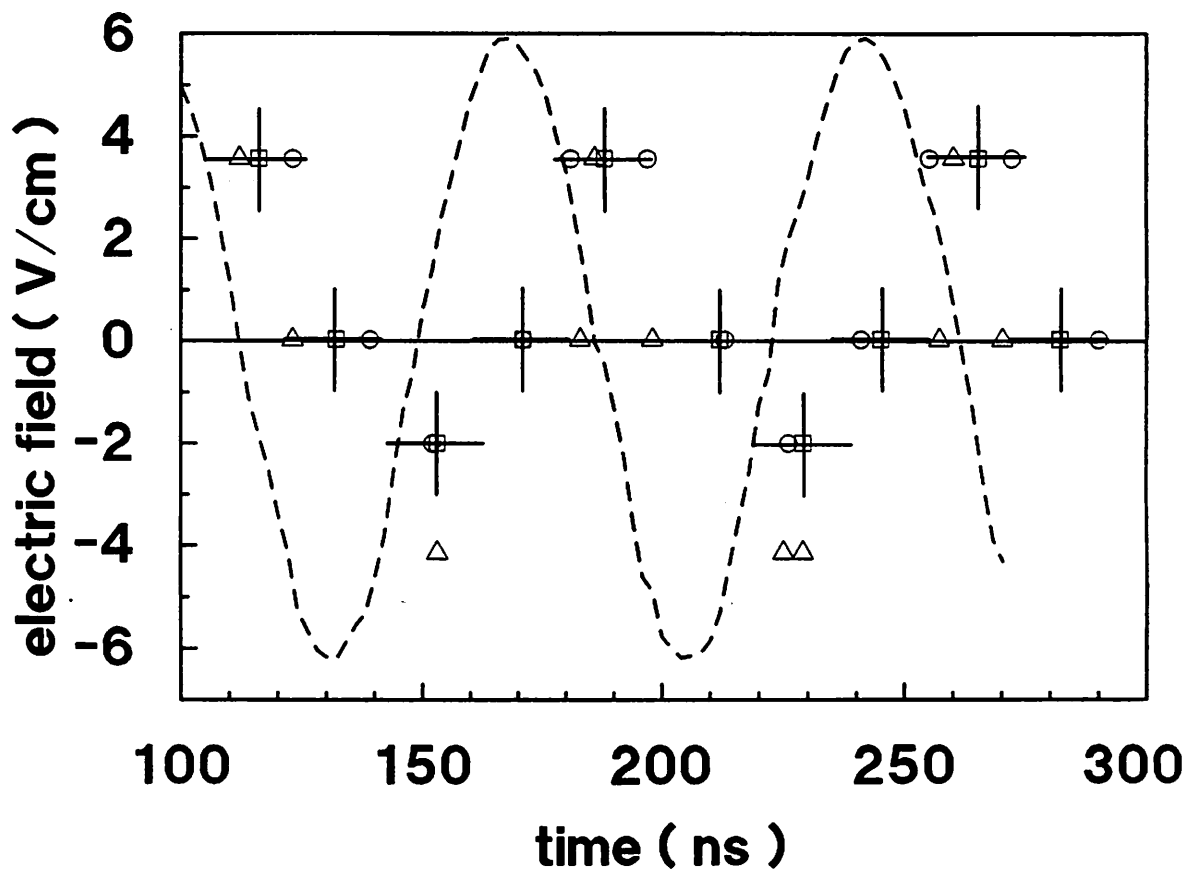


Figure 7

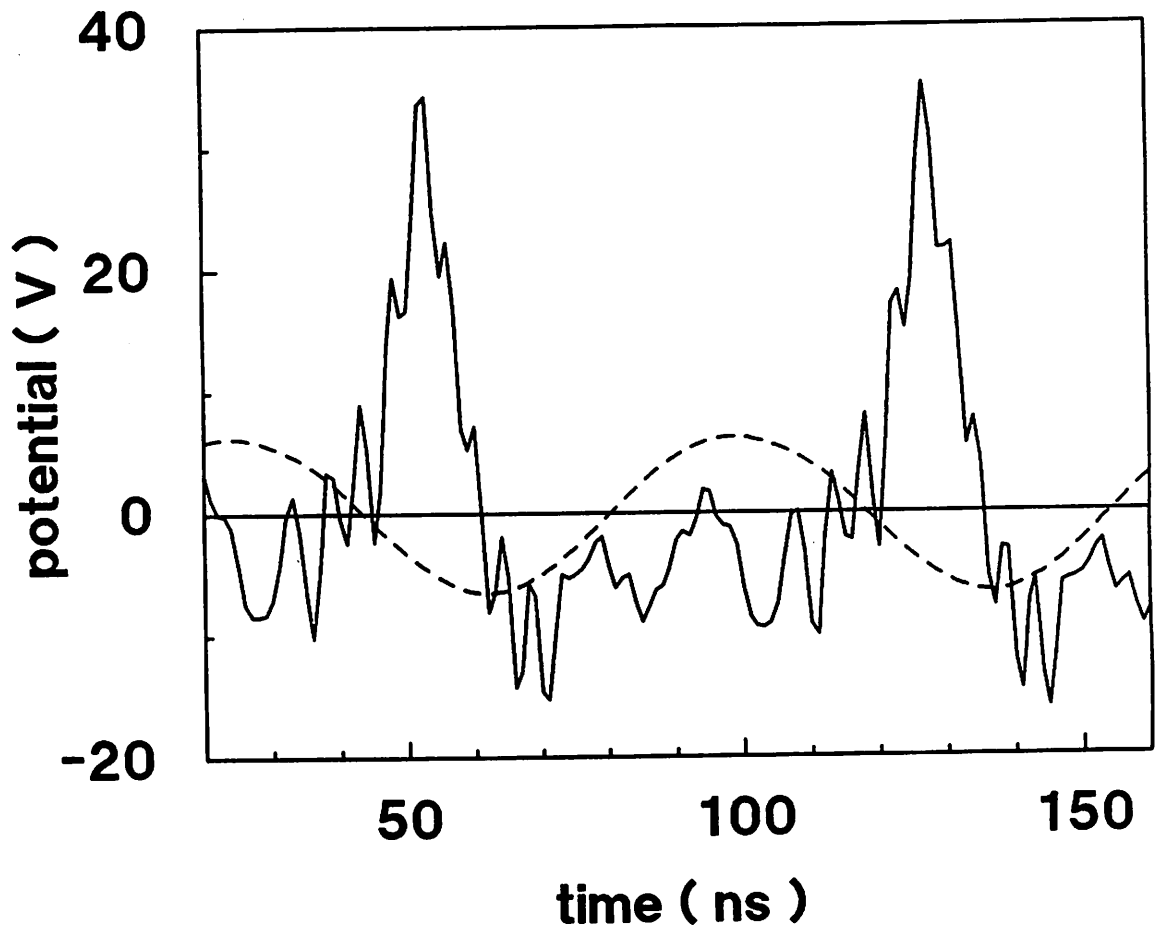


Figure 8

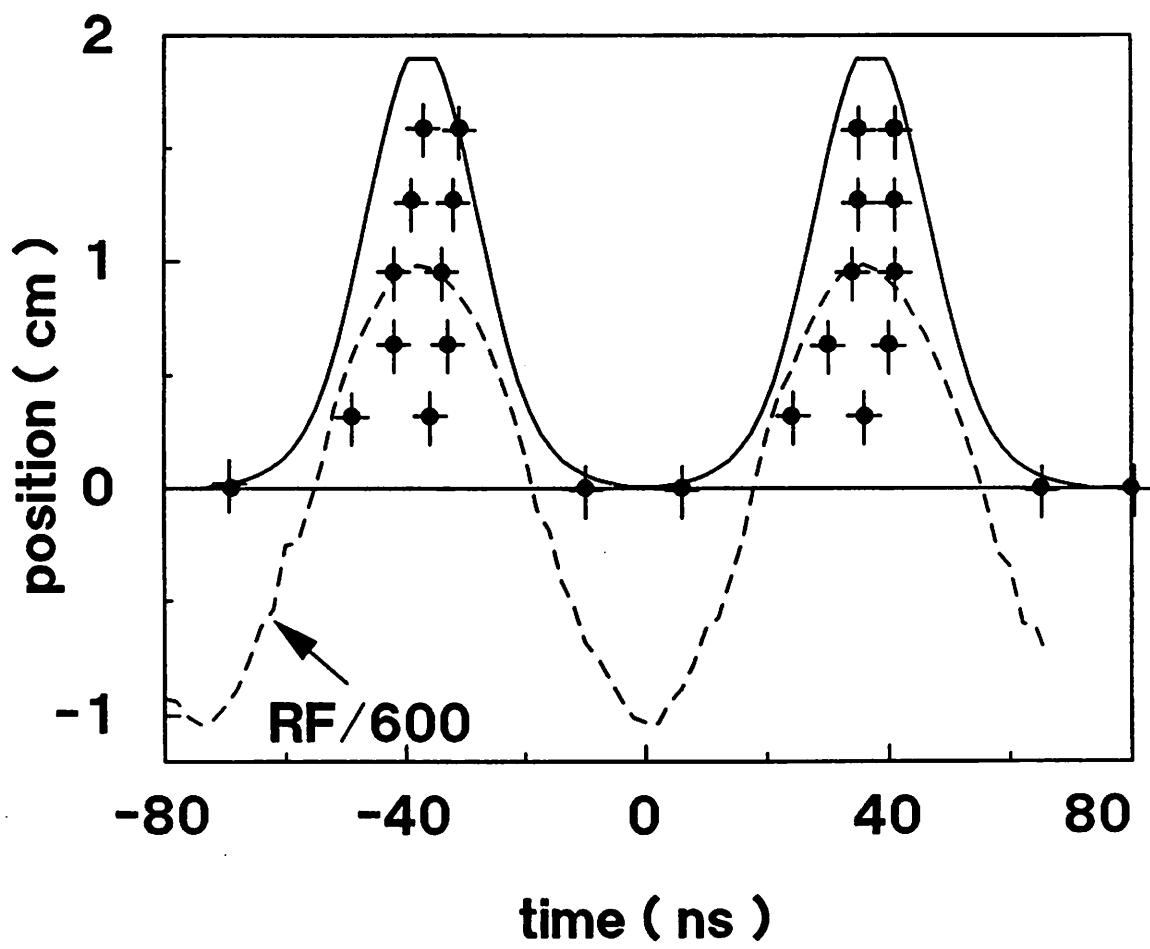


Figure 9

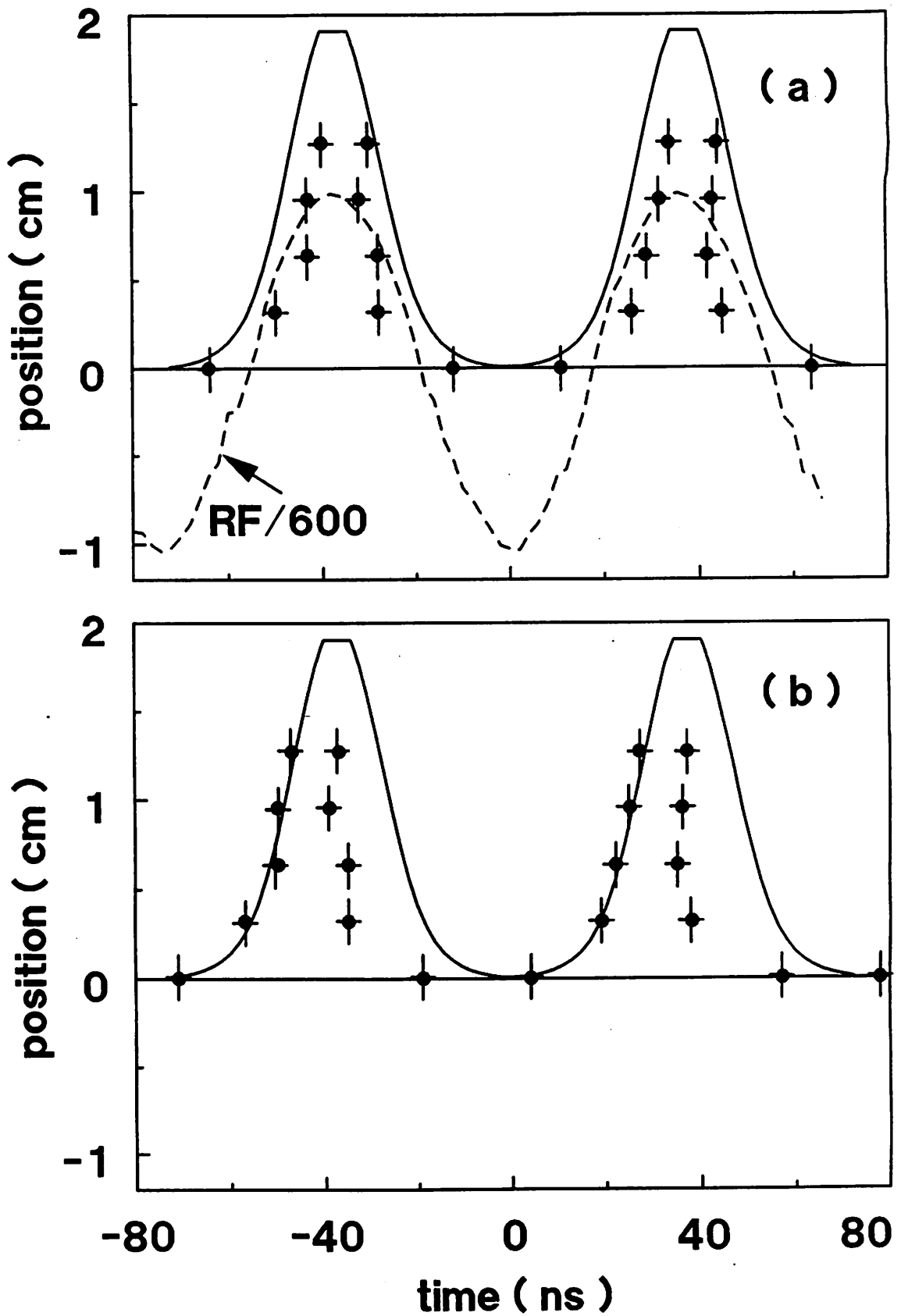


Figure 10